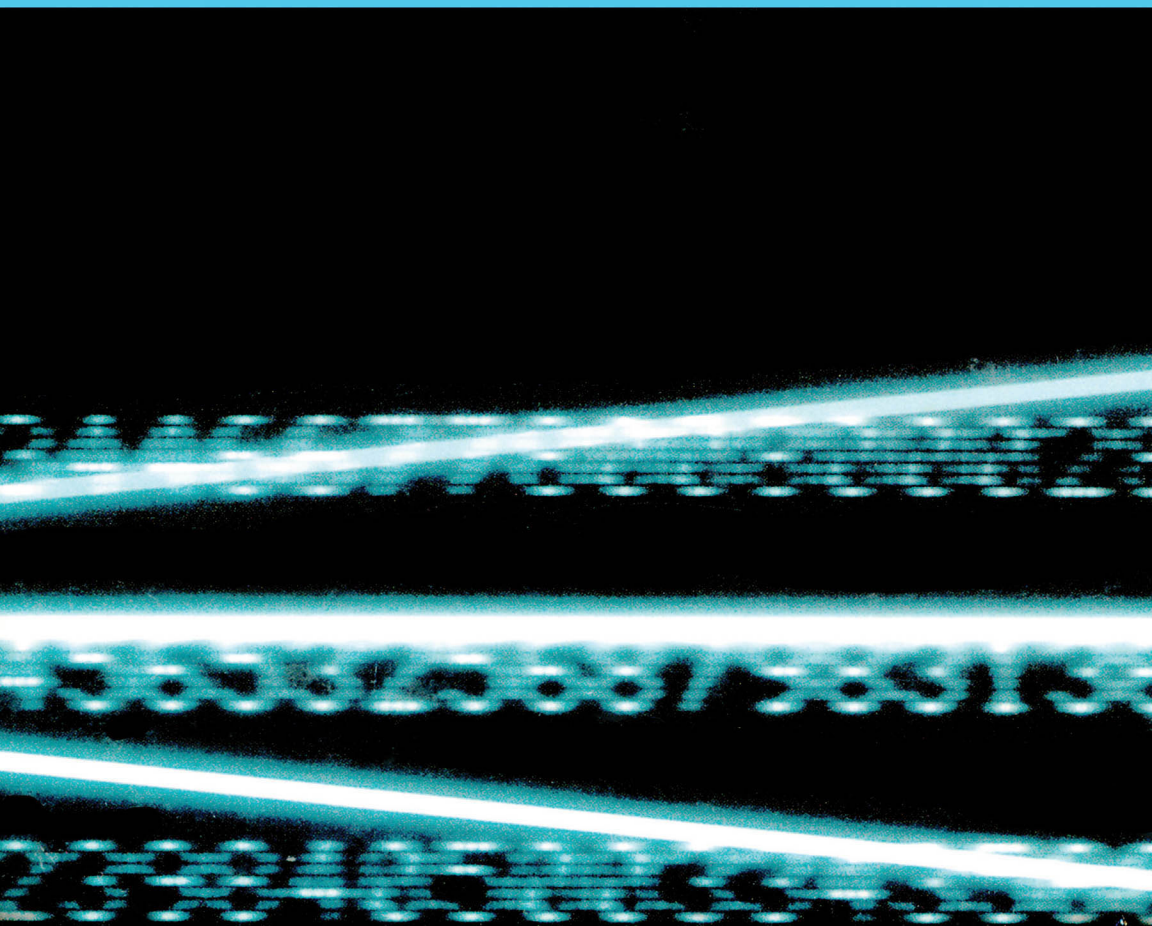


**INTRODUCTION TO  
NITRIDE SEMICONDUCTOR  
BLUE LASERS AND  
LIGHT EMITTING DIODES**

**EDITED BY**

**SHUJI NAKAMURA**

**AND SHIGEFUSA F. CHICHIBU**



 **CRC PRESS**

**Introduction to Nitride  
Semiconductor Blue Lasers  
and Light Emitting Diodes**



Taylor & Francis

Taylor & Francis Group

<http://taylorandfrancis.com>

# **Introduction to Nitride Semiconductor Blue Lasers and Light Emitting Diodes**

Edited by  
Shuji Nakamura  
and Shigefusa F. Chichibu



**CRC PRESS**

---

Boca Raton London New York Washington, D.C.

## **Library of Congress Cataloging-in-Publication Data**

---

Catalog record is available from the Library of Congress

This book contains information obtained from authentic and highly regarded sources. Reprinted material is quoted with permission, and sources are indicated. A wide variety of references are listed. Reasonable efforts have been made to publish reliable data and information, but the authors and the publisher cannot assume responsibility for the validity of all materials or for the consequences of their use.

Neither this book nor any part may be reproduced or transmitted in any form or by any means, electronic or mechanical, including photocopying, microfilming, and recording, or by any information storage or retrieval system, without prior permission in writing from the publisher.

The consent of CRC Press does not extend to copying for general distribution, for promotion, for creating new works, or for resale. Specific permission must be obtained in writing from CRC Press for such copying.

Direct all inquiries to CRC Press, 2000 N.W. Corporate Blvd., Boca Raton, Florida 33431.

**Trademark Notice:** Product or corporate names may be trademarks or registered trademarks, and are used only for identification and explanation, without intent to infringe.

**Visit the CRC Press Web site at [www.crcpress.com](http://www.crcpress.com)**

---

© 2000 by CRC Press

No claim to original U.S. Government works  
International Standard Book Number 0-7484-0836-3  
Printed in the United States of America 3 4 5 6 7 8 9 0  
Printed on acid-free paper

# Contributors

- Daniel L. Barton** Sandia National Laboratories, P.O. Box 5800,  
Albuquerque, NM 87185-1081, USA
- Shigefusa F. Chichibu** Institute of Applied Physics  
University of Tsukuba, 1-1-1 Tennodai, Tsukuba, Ibaraki  
305-8573, Japan
- Steven P. DenBaars** Departments of Materials, Electrical and Computer  
Engineering, University of California, Santa Barbara,  
CA 93106-5050, USA
- Yoichi Kawakami** Department of Electronic Science and Engineering,  
Kyoto University, Yoshida-Honcho, Sakyo-ku, Kyoto  
606-8051, Japan
- Shuji Nakamura** Department of Research and Development,  
Nichia Chemical Industries Ltd. 491 Oka, Kaminaka,  
Anan, Tokushima 774-8601, Japan
- Marek Osinski** Center for High Technology Materials, University of  
New Mexico, 1313 Goddard SE, Albuquerque, NM  
87106, USA
- Fernando A. Ponce** Department of Physics and Astronomy  
Arizona State University, P. O. Box 871504,  
Tempe, AZ 85287-1504, USA
- Takayuki Sota** Department of Electrical, Electronics, and Computer  
Engineering, Waseda University, 3-4-1 Ohkubo,  
Shinjuku, Tokyo 169-8555, Japan
- Masakatsu Suzuki** Central Research Laboratory, Matsushita Electric  
Industrial Co. Ltd. 3-4 Hikaridai, Seika-cho, Souraku-  
gun, Kyoto, 619-02, Japan
- Takeshi Uenoyama** Central Research Laboratory, Matsushita Electric  
Industrial Co. Ltd. 3-4 Hikaridai, Seika-cho, Souraku-  
gun, Kyoto, 619-02, Japan
- Chris G. Van de Walle** Xerox Palo Alto Research Center, 3333 Coyote Hill Road,  
Palo Alto, CA 94304, USA



Taylor & Francis

Taylor & Francis Group

<http://taylorandfrancis.com>

# Preface

Solid-state light-emitting diodes (LEDs) are the ultimate light source. The brightness and durability of solid-state LEDs make them ideal for use in displays and light sources, while semiconductor laser diodes (LDs) have been used in everything from optical communications systems to compact disk players. These applications have been limited, however, by the lack of materials that can efficiently emit blue or green light. For example, full-color displays require at least three primary colors, namely red, green, and blue, to reproduce the visible color spectrum. Such a combination is also needed to make solid-state white-light-emitting devices that would be more durable and consume less power consumption than conventional incandescent bulbs or fluorescent lamps. At present, incandescent bulb lamps and fluorescent lamps are used as light sources for many applications. However, these conventional light sources are old, traditional glass-vacuum-type light sources with poor reliability and durability and a low luminous efficiency. In the past, electronic circuits were made of bulky glass vacuum tubes in spite of poor reliability and durability. However, nowadays all electronic circuits are made with compact highly reliable solid-state semiconductor circuits. Thus, only light sources are not solid-state semiconductors but still made by old, traditional technology.

Recently, however, the development of nitride semiconductors opened the way to obtain all-solid-state semiconductor light sources. For lasers, the shorter the wavelength, the sharper the focused light diameter, which would increase the storage capacity of optical disks. Digital versatile disks (DVDs), which appeared on the market in 1996, rely on red AlInGaP semiconductor lasers and have a data capacity of about 4.7 gigabytes (Gbytes), compared to 0.65 Gbytes for compact disks (CDs) which use infrared lasers. By moving to bluish-purple wavelengths through the use of Nitride semiconductors, the storage capacity can be increased up to 15 Gbytes. Thus, nitride semiconductors are also indispensable for manufacturing semiconductor lasers of next generation DVDs.

The rapid progress of nitride semiconductor devices is extraordinary in comparison with that for other conventional III-V compound semiconductor devices which are made of GaAlAs, InGaAsP, or AlInGaP. For example, the first InGaN-based high-brightness blue LEDs have been put into the market in 1993. Then, InGaN-based quantum-well-structure high-brightness blue and green LEDs appeared in 1995. Now in 1999, these InGaN-based green and blue LEDs are used in many applications, such as LED full-color displays, traffic lights, and white lighting sources. They actually have higher reliability, longer lifetime, and lower power consumption, in comparison to incandescent sources, which will decrease the energy consumption and protect natural resources using the environmentally safe material of nitride semiconductors. Also, amber nitride-based LEDs were developed recently, and the characteristics of these devices are superior to those of conventional amber AlInGaP LEDs, especially for the intensity stability against the ambient temperature. Thus, the only remaining visible color which has not

been developed using nitride semiconductors is red. The luminous efficiency of present InGaN-based green and blue LEDs are 30 and 5 lm/W. That of conventional incandescent bulb lamps is 10 lm/W. Thus, when we make white light using the presently available LEDs, a white LED lamp with a luminous efficiency of 30 lm/W can be fabricated, which is much higher than that (10 lm/W) of the conventional incandescent bulb lamps. Also, there is a great difference in the durability and reliability. The LEDs have an almost indefinite lifetime (longer than 100,000 hours) and superior reliability compared to that of conventional incandescent bulb lamps. Also, the luminous efficiency of blue and green LEDs is still increasing day by day as a result of continuous research efforts such that they will soon catch up with that of fluorescent lamps. Thus, conventional light sources should be replaced with LEDs from the viewpoint of saving energy and natural resources, because of their much longer lifetime, better durability, and higher efficiency. Bluish-purple InGaN-based lasers, which can have the shortest wavelength ever obtained, would have many applications and would cause a major impact in the optoelectronic industry, as did blue and green LEDs. The short wavelength of 400 nm (bluish-purple) means that the light can be focused more sharply, which would increase the storage capacity of optical disks. The first InGaN-based LD under room-temperature (RT) pulsed operation was reported in 1995. In 1996, the first RT continuous-wave (CW) operation was achieved. Then, a lifetime of 10,000 hours was attained in 1998 and LD distribution is started in 1999. The speed of the progress in the research and development of these InGaN-based light-emitting devices is extremely rapid.

The authors of the various chapters were carefully selected as the leaders in the development of the nitride semiconductors and devices. Chapter 1 gives an introductory supplying basic backgrounds in the area of nitride semiconductor blue LEDs and materials. Chapter 2 is for learning a basic lasing theory in semiconductors. Chapters 3 and 4 treat basic problems in nitride semiconductors and quantum well structures such as conductivity control, impurity problems, band offsets, microstructure of imperfection in crystals like threading dislocation, column structure, and polarity problem. In Chapter 5 discussed are emission mechanisms in nitrides which dominate bright emissions from InGaN quantum wells such as quantum well excitons localized at the potential minima produced by the alloy compositional fluctuations in InGaN. In Chapters 6 and 7, degradation mechanisms of InGaN devices are discussed. Finally, current performance of blue LEDs and LDs are described.

This book is to be used as a textbook for postgraduate courses, professional engineers or scientists wishing to learn the latest progress in nitride semiconductors and related optical devices.

The editors wish to thank most warmly the authors and publishers who have contributed to this book. Voluntary help of T. Mizutani and M. Sugiyama in the editorial procedures is appreciated. We also wish to express our appreciation to our wives for continuous encouragements.

May 1, 1999

Nichia Chemical Industries      Shuji Nakamura  
University of Tsukuba      Shigefusa F. Chichibu

# Contents

<b>1. Basics Physics and Materials Technology of GaN LEDs and LDs.</b>	<b>1</b>
Steven P. DenBaars	
1.1 Introduction	1
1.1.1 Historical Evolution of LED Technology	1
1.2 Basic Physics of LEDs: Injection Luminescence	3
1.2.1 Direct and Indirect Band-Gap Material	4
1.2.2 Radiative Recombination	5
1.2.3 External Quantum Efficiency	7
1.2.4 Luminous Efficiency	8
1.2.5 Injection Efficiency	9
1.2.6 Heterojunction vs. Homojunction LED Materials	10
1.2.7 Quantum Well LEDs	12
1.3 LED Materials Selection	12
1.3.1 Energy Band Structure/Lattice Constants	12
1.3.2 GaN Physical Properties	13
1.3.3 GaN Based LED Structures	13
1.4 Crystal Growth	15
1.4.1 MOCVD Growth	15
1.4.2 MOCVD Systems for Production	17
1.4.3 Molecular Beam Epitaxy (MBE)	18
1.4.4 Chloride Vapor Phase Epitaxy	19
1.5 Group-III Nitride Materials Growth Issues	20
1.5.1 Substrates	20
1.5.2 Nucleation Layer Technology	21
1.5.3 Growth and Doping of GaN	21
1.5.4 Growth of AlGaIn and AlGaIn/GaN Heterostructures	22
1.5.5 Growth of InGaIn and InGaIn/GaN Heterostructures	23
1.6 Conclusions	24
1.7 References	25
<b>2. Theoretical Analysis of Optical Gain Spectra</b>	<b>29</b>
Takeshi Uenoyama and Masakatsu Suzuki	
2.1 Introduction	29
2.2 Optical Gains Spectra by Many-Body Approach	30
2.2.1 Linear Response Theory	30

2.2.2 Screening Effects . . . . .	32
2.2.3 Self-Energies of Electron Gas . . . . .	34
2.2.4 Coulomb Enhancement . . . . .	36
2.3 Electronic Band Structures . . . . .	39
2.3.1 Electronic Band Structures of Bulk GaN and AlN . . . . .	39
2.3.2 Strain Effect on Electronic Band Structures . . . . .	42
2.3.3 k·p Theory for Wurtzite . . . . .	43
2.3.4 Physical Parameters . . . . .	44
2.3.5 Subband Structures of GaN/AlGaIn Quantum Wells . . . . .	47
2.3.6 Subband in Wurtzite Quantum Wells . . . . .	47
2.4 Optical Gain Spectra of III-V Nitrides LD Structures . . . . .	49
2.4.1 Free Carrier Model . . . . .	49
2.4.2 Coulomb Enhancement (Excitonic Effects) in the Optical Gain . . . . .	56
2.4.3 Optical Gain with Localized States . . . . .	58
2.5 Conclusions . . . . .	63
2.6 References . . . . .	64
<b>3. Electrical Conductivity Control . . . . .</b>	<b>67</b>
Chris G. Van de Walle	
3.1 Doping . . . . .	67
3.1.1 Theory of Native Defects and Impurities . . . . .	68
3.1.2 n-type Doping . . . . .	75
3.1.3 p-type Doping . . . . .	81
3.2 Band Offsets . . . . .	90
3.2.1 Theory of Band Offsets at Nitride Interfaces. . . . .	91
3.2.2 Experimental Results for Band Offsets . . . . .	95
3.2.3 Discussion . . . . .	96
3.3 Acknowledgments . . . . .	97
3.4 References . . . . .	97
<b>4. Crystal Defects and Device Performance in LEDs and LDs . . . . .</b>	<b>105</b>
Fernando A. Ponce	
4.1 Crystal Growth and Microstructure . . . . .	105
4.1.1 Lattice Structure of the Nitride Semiconductors . . . . .	106
4.1.2 Thin Film Epitaxy and Substrates . . . . .	107
4.2 Epitaxy on SiC Substrates . . . . .	109
4.3 Epitaxy on Sapphire Substrates . . . . .	111
4.3.1 AlN as a Buffer Layer . . . . .	113
4.3.2 GaN as a Buffer Layer . . . . .	114
4.4 Homoepitaxial Growth of GaN . . . . .	115
4.5 Defect Microstructure in LEDs and LDs. . . . .	116
4.5.1 Large Defect Densities in High Performance Materials . . . . .	117
4.5.2 Columnar Structure of GaN on Sapphire . . . . .	119
4.5.3 Tilt Boundaries . . . . .	121

4.5.4 Twist Boundaries . . . . .	122
4.6 Polarity and Electronic Properties . . . . .	123
4.7 The Nature of the Dislocation . . . . .	126
4.7.1 Determination of the Burgers Vector . . . . .	126
4.7.2 Nanopipes and Inversion Domains . . . . .	129
4.8 Spatial Variation of Luminescence . . . . .	132
4.8.1 Undoped Material. . . . .	132
4.8.2 Doped Materials . . . . .	135
4.9 Microscopic Properties of $\text{In}_x\text{Ga}_{1-x}\text{N}$ Quantum Wells . . . . .	136
4.9.1 The Nature of the InGaN/GaN Interface . . . . .	137
4.9.2 Microstructure of Quantum Wells . . . . .	139
4.9.3 Spatial Variation of the luminescence of $\text{In}_x\text{Ga}_{1-x}\text{N}$ Quantum Wells . . . . .	144
4.10 Microstructure and Device Performance . . . . .	149
4.10.1 Stress and Point Defect Structure . . . . .	149
4.10.2 Minimization of Strain by Maximizing Film Smoothness. . . . .	149
4.10.3 The Role of Dislocations in Strain Relaxation . . . . .	150
4.10.4 The Role of Nanopipes and Extension to ELOG Structures . . . . .	150
4.11 References . . . . .	150

**5. Emission Mechanisms and Excitons in GaN and InGaN Bulk and QWs** 153

Shigefusa F. Chichibu, Yoichi Kawakami, and Takayuki Sota

5.1 Introduction . . . . .	153
5.2 GaN Bulk Crystals. . . . .	154
5.2.1 Free and Bound Excitons . . . . .	154
5.2.2 Biexcitons in GaN . . . . .	165
5.2.3 Strain Effects . . . . .	175
5.2.4 Phonons in Nitrides . . . . .	176
5.3 InGaN Bulk and QWs for Practical Devices . . . . .	184
5.3.1 Quantized Energy Levels . . . . .	186
5.3.2 Piezoelectric Field . . . . .	192
5.3.3 Spontaneous Emission of Localized Excitons . . . . .	197
5.3.4 Localized Exciton Dynamics . . . . .	219
5.3.5 Optical Gain in Nitrides . . . . .	248
5.4 References . . . . .	258

**6. Life Testing and Degradation Mechanisms in InGaN LEDs** . . . . . 271

Marek Osinski and Daniel L. Barton

6.1 Introduction . . . . .	271
6.2 Life Testing of InGaN/AlGaIn/GaN LEDs . . . . .	272
6.2.1 Life Testing Primer . . . . .	272
6.2.2 Potential Degradation Regions in LEDs . . . . .	273
6.2.3 Life Test System Considerations . . . . .	274
6.2.4 Results of Life Tests on Nichia Blue InGaN/AlGaIn/GaN	

Double Heterostructure LEDs . . . . .	276
6.3 Analysis of Early Test Failures . . . . .	281
6.3.1 Analysis of LED #19 . . . . .	281
6.3.2 Analysis of LEDs #16 and 17 . . . . .	282
6.4 Effects of UV Emission on Plastic Transparency . . . . .	286
6.5 Thermal Degradation of Plastic Package Transparency . . . . .	289
6.6 Degradation of GaN-Based LEDs Under High Current Stress . . . . .	295
6.7 Double Heterostructure Device Testing . . . . .	295
6.8 EBIC Analysis . . . . .	301
6.9 Pulsed Current Stress Experiments and Results on Quantum Well LEDs . . . . .	307
6.10 Failure Analysis of Degraded Quantum Well LEDs . . . . .	309
6.11 Discussion . . . . .	312
6.12 Summary . . . . .	313
6.13 References . . . . .	314
<b>7. Development and Future Prospects of GaN-based LEDs and LD . . . . .</b>	<b>317</b>
Shuji Nakamura	
7.1 Properties of InGaN-based LEDs . . . . .	317
7.1.1 Introduction . . . . .	317
7.1.2 Amber LEDs . . . . .	317
7.1.3 UV/Blue/Green LEDs . . . . .	321
7.1.4 Roles of Dislocations in InGaN-Based LEDs . . . . .	328
7.2 LDs Grown on Sapphire Substrate . . . . .	333
7.2.1 Introduction . . . . .	333
7.2.2 LDs Grown on Sapphire Substrates . . . . .	333
7.2.3 ELOG Substrate . . . . .	336
7.2.4 InGaN-Based LDs Grown on ELOG Substrates . . . . .	338
7.3 LDs Grown on GaN Substrate . . . . .	343
7.3.1 Free-Standing GaN Substrates . . . . .	344
7.3.2 Characteristics of LDs . . . . .	344
7.4 Future Prospects of InGaN-based Emitting Devices . . . . .	348
7.5 References . . . . .	348
<b>Appendix</b>	
Parameters Table . . . . .	351
Subject Index . . . . .	369

# Chapter 1

## Basics Physics & Materials Technology of GaN LEDs and LDs

Steven P. DenBaars

### 1.1 INTRODUCTION

Recently, the Group-III nitride based semiconductors have emerged as the leading material for the production of blue LEDs and blue laser diodes. Nature has blessed the  $(\text{In}_x\text{Ga}_{1-x})_y\text{Al}_{1-y}\text{N}$  alloy system with a continuous and direct bandgap semiconductor alloy spanning ultraviolet to blue/green/yellow wavelengths. As we will learn in this chapter the direct bandgap semiconductor is perhaps the most efficient means to generate light from electricity. The purpose of this chapter is to review the basic physics of LEDs, materials selection, epitaxial growth, and describe the historical evolution of technologies employed in the manufacturing of LEDs and laser diodes.

#### 1.1.1 Historical Evolution of LED Technology

The achievement of bright blue InGaN LEDs has basically led to a revolution in LED technology and opened up enormous new markets that were not accessible before. The remarkable advancements in GaN based LED materials depended on several key breakthroughs in materials synthesis and fabrication. The lack of p/n junctions in the Group-III nitrides and poor crystal quality slowed research for many decades. The use of InGaN/GaN double heterostructure (DH) in LEDs in 1994 by Nakamura (Nakamura *et al.*, 1994a) and achievement of p-doping in GaN by Akasaki (Amano *et al.*, 1990a) is widely credited with reigniting the III-V nitride system. It has taken over twenty years since the first optical pumped stimulated emission was observed in GaN crystal (Dingle *et al.*, 1994) and first LEDs (Pankove *et al.*, 1971) were fabricated to come to the recent realization of blue lasers. In the late 1980s remarkable progress for high brightness LEDs for displays occurred. This remarkable revolution in LED performance for the commercially important compound semiconductors materials system is illustrated in Figure 1.1. Notable progress is the development of high efficiency AlGaAs, AlGaInP, and AlGaInN alloys. In particular, the efficiency of p/n GaN LEDs increased rapidly after the first reports of p/n junctions by Akasaki in 1989. This

was caused primarily by the higher efficiency afforded by heterojunction based LEDs.

The advances in GaN and GaAs based LEDs has enabled many new markets to be opened for LEDs. For many years solid state device researchers have dreamed of obtaining a bright blue light source. Only now can one use three LEDs to tune to any color in the visible range, or even use a single blue LED in combination with phosphors to make "white LEDs". This concept is particularly attractive because the solid state nature of semiconductor devices produce very high reliability. The average lifespan of an LED is of the order of tens of years (Craford, 1977). Full-color and white LEDs are now appearing in numerous applications ranging from outdoor TVs, traffic signals, scanners, flashlights, and automotive backlighting. Another potentially large application of GaN is in fabricating blue laser diodes (LDs) for extremely high-density optical storage systems. Because the storage density of optical compact discs (CDs) and digital video discs (DVDs) is inversely proportional to the square of the laser wavelength a 4-8 fold increase in capacity could be realized with short wavelength laser diodes. Future research is needed to commercialize GaN for optical storage, energy efficient lighting, communications, printing, projection TV, and even surgery. As GaN manufacturing volumes increase and costs decrease one can expect to see GaN LEDs and LDs in ever increasing applications wherever economical and reliable illumination is needed.

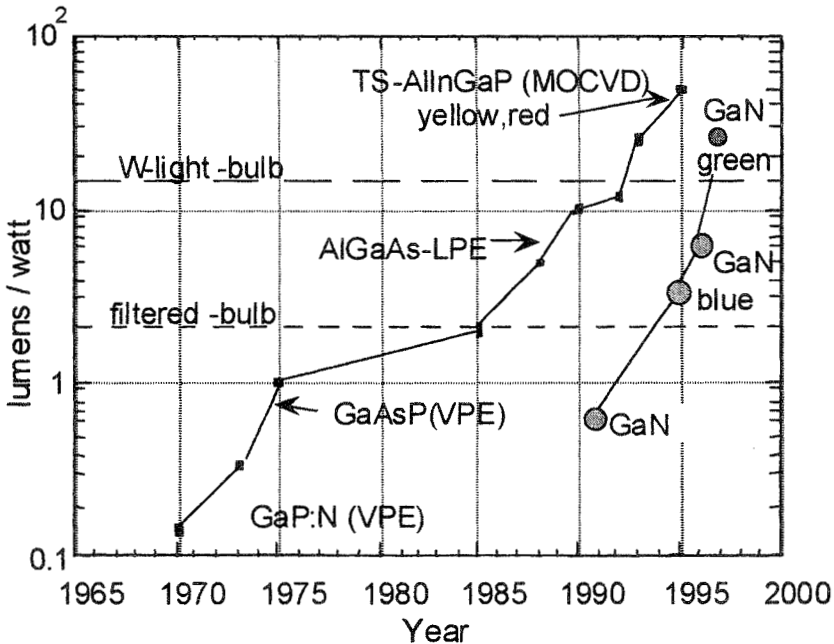


Figure 1.1 Evolution of LED performance (lumens/watt) for the commercially important materials.

## 1.2 BASIC PHYSICS OF LEDs: INJECTION LUMINESCENCE

In order to better understand GaN LEDs it is important to understand the physics governing light emission in semiconductors. Light emitting diodes (LEDs) are a class of diodes that emit spontaneous radiation under suitable forward bias conditions. LEDs are fabricated from semiconductor materials in which a p/n junction is fabricated. Injection electroluminescence (EL) is the most important mechanism for exciting the semiconductor materials. Under forward bias conditions, electrons are injected into the p-type semiconductor and holes are injected into the n-type material. Recombination of these minority carriers with the majority carriers at the p/n junction results in near bandgap radiation. The wavelength of the emitted light is governed by the energy bandgap of the semiconductor material, and is given as:

$$\lambda = \frac{1.24}{E_{\text{gap}}} [\mu\text{m}] \quad (1.1)$$

A schematic representation of a radiative recombination in a forward bias p/n junction is shown in Figure 1.2. In GaN the p-type material is fabricated from Mg-doped GaN and the n-type material is silicon doped GaN. Prior to 1989 only materials emitting radiation covering the green through infrared spectrum existed. The first visible LEDs were red GaAsP emitters invented at General Electric by Holnyak and Bavacqua in 1962 (Holnyak *et al.*, 1962). Blue was the missing primary color (red, green and blue) and as such full-color emission could not be achieved. Therefore with the advent of the GaN system the full-visible color spectrum is now accessible for the first time.

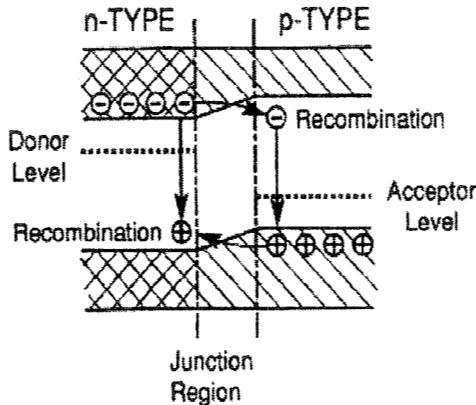
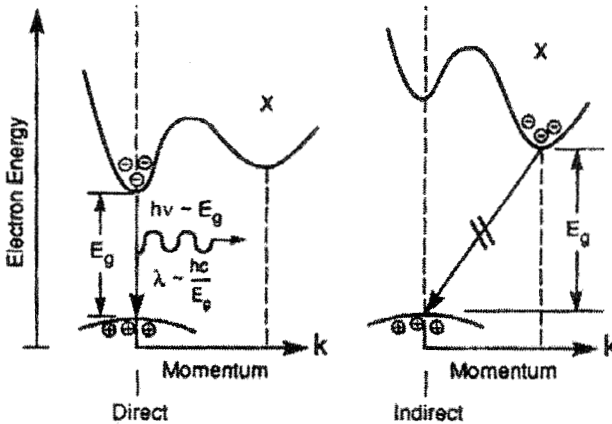


Figure 1.2 Schematic representation of a p/n junction in a light emitting diode under forward bias.

### 1.2.1 Direct and Indirect Band-Gap Material

Semiconductor LED materials can be divided into two different classes of band structure, exhibiting either direct or indirect bandgap behavior. In a direct bandgap semiconductor, electrons in conduction band minima and holes in the valence band maxima have the same momentum as shown in Figure 1.3. The probability of a band-to-band radiative transition for the direct bandgap semiconductor is high since momentum will be conserved upon recombination. In contrast, in an indirect bandgap semiconductor the electrons in the conduction band minima have different momentum from the holes in the valence band maxima, and therefore momentum is not conserved. In an indirect semiconductor an electron would have to change its momentum before recombining with a hole. A third component, a phonon, is required to participate in the recombination event for the electron to change its momentum and a transition to occur in the indirect gap semiconductor. This results in a significantly lower recombination probability for a band-to-band transition to occur in the indirect gap semiconductor. This fact is especially evident when comparing direct bandgap GaN to indirect SiC LEDs. GaN LEDs exhibit quantum efficiencies as high as 12%, which is significantly higher than the 0.02% observed in SiC LEDs.



**Figure 1.3** Energy band diagram of direct (GaN) and indirect bandgap (SiC) semiconductors. Electron energy is plotted versus momentum,  $k$ .

### 1.2.2 Radiative Recombination

Electron-hole recombination can be either radiative or non-radiative. These two recombination pathways can be considered as parallel processes occurring across the energygap of the semiconductor, as illustrated in Figure 1.4. Maximizing the probability for radiative recombination and decreasing the probability for non-radiative recombination paths can increase light output from an LED. Several mechanisms cause non-radiative recombination in semiconductors, among these are; auger recombination, recombination at defect sites, and multiphonon emission at deep impurity sizes (Henry *et al.*, 1976). Radiative transitions in semiconductors occur primarily by interband transitions, excitonic recombination, or recombination through impurity centers.

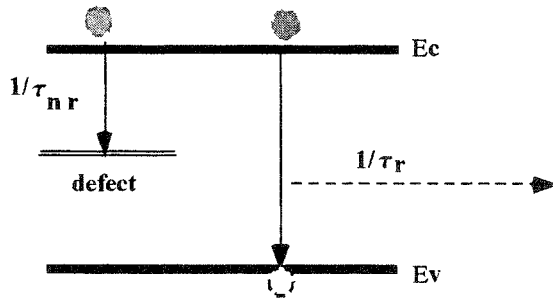


Figure 1.4 Schematic illustration of radiative and non-radiative transition in a semiconductor.

Under continuous injection of carriers an excess carrier density will exist in the semiconductor. For charge neutrality to exist the excess electrons “ $\Delta N$ ” and excess holes “ $\Delta P$ ” must be equal after injection ceases; the excess carrier density has been found to decrease exponentially with time with a characteristic lifetime:

$$\Delta N = \Delta N_0 \exp(-t/\tau) \tag{1.2}$$

where  $\Delta N_0$  = initial excess carrier concentration, and

$t$  = recombination lifetime.

The recombination lifetime consists of both a radiative lifetime and a non-radiative lifetime

$$\frac{1}{\tau} = \frac{1}{\tau_r} + \frac{1}{\tau_{nr}} \tag{1.3}$$

The radiative recombination rate is defined with the excess carrier density and recombination lifetime as (Kressel *et al.*, 1977a):

$$R_r = \frac{\Delta n}{\tau_r} \tag{1.4}$$

Likewise the non-radiative recombination rate:

$$R_{nr} = \frac{\Delta n}{t_{nr}}. \quad (1.5)$$

The internal radiative quantum efficiency is defined as the ratio of the rate of radiative recombination to the total recombination rate:

$$\eta_i = R_r / (R_r + R_{nr}). \quad (1.6)$$

Therefore, the internal quantum efficiency can be expressed in terms of the radiative and non-radiative lifetimes.

$$\eta_i = \frac{1/t_r}{1/t_r + 1/t_{nr}} = \frac{1}{1 + t_r/t_{nr}}. \quad (1.7)$$

By keeping  $t_r/t_{nr}$  small a maximum internal quantum efficiency can be obtained. This is done by making  $t_{nr}$  long compared to  $t_r$ . Growing materials with low defect densities and eliminating impurities that cause non-radiative deep levels are certain material properties that increase the quantum efficiency. Typical GaP and GaAs based LEDs must be manufactured with lower than  $10^4$  defects  $\text{cm}^{-2}$  in order to achieve reasonable efficiencies. One apparent exception to this rule is that GaN LEDs still emit light efficiently despite exhibiting defect densities as high as  $10^{10} \text{cm}^{-2}$  (Lester *et al.*, 1995). Using the principle of detailed balance, (Shockley, 1950) in which at equilibrium the rate of optical generation of electron-hole pairs is equal to their rate of radiative recombination, the spontaneous recombination rate for band-to-band emission can be expressed as:

$$R_{sp} = B_r np. \quad (1.8)$$

Where  $B_r$  ( $\text{cm}^3/\text{s}$ ) is the radiative recombination coefficient. Under non-equilibrium conditions additional carriers are introduced into the material and the spontaneous recombination rate occurs. At high injection levels, the excess carrier density will substantially exceed the background concentration:

$$\Delta n > p_o + n_o, \quad (1.9)$$

so that the average carrier lifetime can be expressed as:

$$t_r \cong \frac{1}{B_r \Delta n}, \quad (1.10)$$

which occurs in the ‘‘bimolecular’’ recombination region. In the case of bimolecular recombination, the lifetime value is continually changing so  $t_r$  represents the average carrier lifetime. The other region for the lifetime occurs at low injection levels in which the excess carriers decay exponentially with time. In this region the lifetime can be determined by the background carrier concentration:

$$t_r \cong \frac{1}{B_r(p_o + n_o)} \tag{1.11}$$

For n-type material  $n_o \gg p_o$ :

$$t_r \cong \frac{1}{B_r n_o} \tag{1.12}$$

Likewise, for p-type material

$$t_r \cong \frac{1}{B_r p_o} \tag{1.13}$$

For intrinsic material at low injection levels the longest possible lifetime is found

$$t_r \cong \frac{1}{2B_r n_i} \tag{1.14}$$

Interface recombination is another factor that effects the effective lifetime and is taken into account by dividing the average non-radiative interface recombination velocity  $S$  by the active layer thickness  $d$ . The effective lifetime is then a combination of all the competing process lifetimes:

$$\frac{1}{t_{eft}} = \frac{1}{t_{nr}} + \frac{2S}{d} + B_r(n_o + p_o) \tag{1.15}$$

Since interfaces occur on each side of the active region in DH and SQW LED, two multiplies the interface recombination velocity.

### 1.2.3 External Quantum Efficiency

The best measure for LED efficiency is how much light is generated for the injected current. Because of the direct bandgap in GaN most carriers recombine through the radiative pathway and quantum efficiencies as high as 10% are achieved. Fundamentally, the external quantum efficiency can be expressed as the ratio of photons out per injected electron:

$$\eta_{ext} = ( \text{photons - out} ) / ( \text{photons - in} ) \tag{1.16}$$

The external quantum efficiency is product of material and optical coupling efficiency given as:

$$\eta_{ext} = \eta_{inj} \eta_i \eta_{opt} \tag{1.17}$$

where  $\eta_{inj}$  is the injection efficiency and  $\eta_i$  is the light generation efficiency, and  $\eta_{opt}$  is the optical or light extraction efficiency. Since light generation is predominantly generated on the p-side of the diode for GaP (Kressel *et al.*, 1977c) and AlGaAs (Varon *et al.*, 1981), a high electron injection efficiency is typically

desired. This dictates that high injection efficiency will be achieved if the electron current dominates over the hole current.

For a material to be an efficient visible light emitter it should meet three important criteria, namely (1) possess an efficient radiative pathway, (2) have an energy gap of appropriate width, (3) and be controllably doped both p and n-type with low resistivities. The most important materials system that has had great technological success in meeting these demands is the III–V semiconductors and their alloys. Table 1.1 summarizes the commercially important visible LED materials and the external quantum efficiencies achieved in each system currently achievable.

**Table 1.1** Summary of Commercially Available Visible LED Materials

Material	Color Range	Peak Emission	Luminous Efficiency (lm/w)	External Quantum Eff. (%)	Growth Technique	Device Type
AlGaInP	Red	636nm	35	24%	MOCVD	DH
AlGaAs	Red	650 nm	8.0	16%	LPE	DH
AlGaInP	Amber	590nm	40	10%	MOCVD	DH
InGaN	Blue	470nm	10	11%	MOCVD	QW
InGaN	Green	520nm	34	10%	MOCVD	QW
InGaN	UV	372nm	0	7.5%	MOCVD	DH
InGaN	Amber	590nm	14	3.5%	MOCVD	QW
ZnSe	Blue	512 nm	17	5.3%	MBE	DH
GaP:Zn-O	Red	650 nm	4.0	5.0%	LPE	H
GaP:N	Yellow-Green	565 nm	1.8	0.3%	LPE	H
GaAsP:N	Yellow	590 nm	1.0	0.3%	VPE	H
SiC	Blue	470 nm	0.02	0.02%	CVD	H

DH = Double Heterostructure, H = Homojunction Device, QW = Quantum Well

#### 1.2.4 Luminous Efficiency

The luminous efficiency is expressed in lumens per watt. The term luminous efficiency refers to the energy conversion efficiency of the light source in converting electrical power into light we can see, luminous flux. To calculate the luminous efficiency we multiply the radiant power efficiency by the luminous efficacy factor which is wavelength dependent and peaks at 683 lumens/watt at 555 nm. The CIE luminosity curve for the visible wavelength range is shown in Figure 1.5 below, the solid line representing the luminous efficiency for a 100% efficient emitter. As is evident from this curve GaN and AlGaInP LEDs is exceeding the efficiency of incandescent light sources in the red to green regions of

the spectra. By further improving the external quantum efficiencies of the III-V semiconductors we can expect that LEDs will one day be the most efficient light sources available.

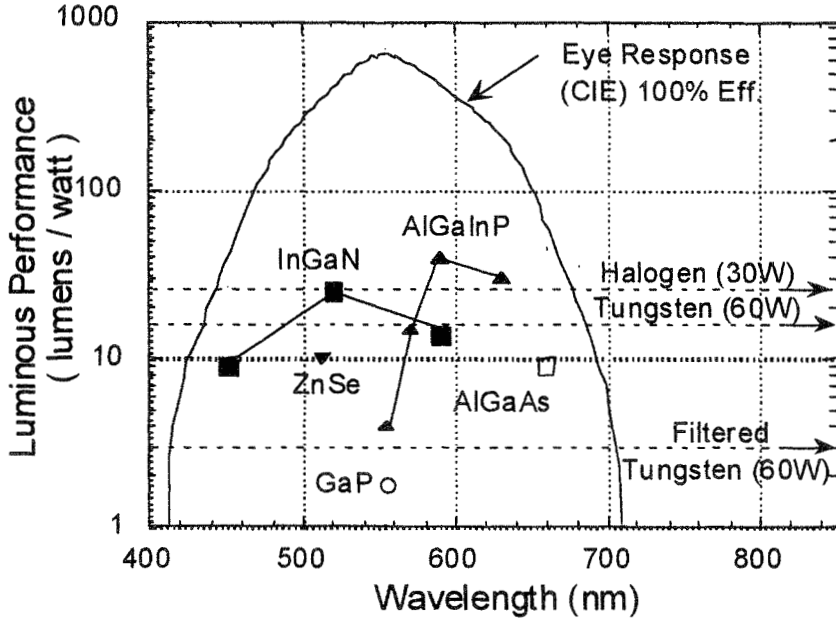


Figure 1.5 Luminous Efficiencies of LEDs over the visible range.

### 1.2.5 Injection Efficiency

The external efficiency is also influenced by the carrier injection efficiency into the active region. For injection into a p-semiconductor the injection efficiency is defined as the ratio of the electron current  $J_e$  to the total forward current  $J_f$  and can be expressed as:

$$n_{inj} = \frac{J_e}{J_e + J_h} = \frac{J_e}{J_f} \tag{1.18}$$

From p-n junction theory (Shockley, 1950) we can define the injection efficiency in terms of relevant materials properties:

$$n_{inj} = \frac{D_n n_p L_p}{D_n n_p L_p + D_p p_n L_n} \tag{1.19}$$

where  $D_n$  and  $D_p$  are the diffusion coefficients for electrons and holes, respectively.  $L_p$  and  $L_n$  are the minority carrier diffusion lengths, and  $n$  and  $p$  are the net electron and hole concentrations on the two sides of the junction. Typically in GaAs minority carrier diffusion lengths are one micron or more. In the nitrides the diffusion lengths are potentially much smaller. At thermal equilibrium the net electron and hole concentration can be expressed with the doping level of donors  $N_D$  and acceptors  $N_A$ :

$$n = n_i^2 / N_A, \quad (1.20)$$

and

$$p = n_i^2 / N_D. \quad (1.21)$$

Therefore to obtain a high injection efficiency we want to adjust the doping such that  $N_D > N_A$ . However, to optimize the optical efficiency the material must be kept transparent by light generated at the junction. Therefore free carrier absorption must be minimized by lowering the doping level in the heavily doped n-type material to below  $10^{18} \text{ cm}^{-3}$  (Varon *et al.*, 1981).

### 1.2.6 Heterojunction vs. Homojunction LED Materials

Both homojunction and heterojunction semiconductor structures can be employed for visible LEDs. By combining wide bandgap semiconductors with narrow bandgap semiconductor a “heterojunction” is formed and extremely desirable properties unattainable in homostructures become possible (Kroemer, 1963). In homojunction LEDs, the p and n materials are composed of the same energy gap semiconductor, while in heterojunction LEDs two materials of different bandgap are utilized. A typical GaAsP LED consists of a homojunction with a diffused p/n junction. Since the GaAsP is grown on an absorbing GaAs substrate only light emitted upwards from the junction escapes. This so called “bandgap engineering” (Capasso *et al.*, 1989) allows the LED designer to achieve higher luminous efficiencies than conventional homostructures. The two major benefits of heterostructure LEDs are the increased minority carrier injection efficiency and the ability to use wide-gap material. The wide-bandgap layers are transparent to the light generated in the narrow gap active layer and therefore do not contribute to photon reabsorption. The radiative efficiency in heterostructure LEDs is higher than homostructure LEDs because of the increased current injection efficiency at the heterojunction. In particular, since the radiative efficiency of the p-side is usually much higher than the n-side, higher efficiency devices are made by eliminating the minority carrier injection into the n-type material. By creating a heterostructure at the p/n interface a valence band discontinuity is formed which provides a hole potential barrier. By adding an additional heterostructure confinement at the other side of the active layer increases because the second heterointerface prevents the injected electrons from diffusing out of the narrow-gap layer.

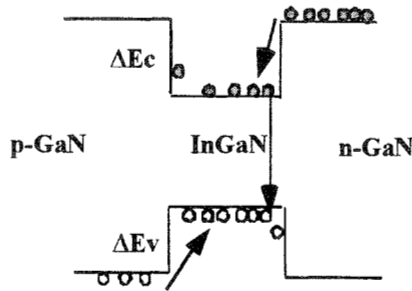


**Figure 1.6** Energy band diagram for a heterojunction. LEDs in which the conduction band discontinuity  $\Delta E_c$  and Valence band discontinuity  $\Delta E_v$  provide a barrier to confine carriers into active region.

Figure 1.6 illustrates the energy band diagram for heterojunction flat-band conditions where the applied bias just cancels the built in field. For heterojunctions the bandgap discontinuity affords a significant improvement in the injection efficiency. The conduction band discontinuity  $\Delta E_c$  and the valence band discontinuity  $\Delta E_v$ , produce a barrier to electron and hole flow, respectively. For a p-n heterojunction the ratio of electron to hole current can be expressed as (Casey *et al.*, 1978):

$$\frac{J_e}{J_h} = \frac{D_n n_p L_p}{D_p p_n L_n} \tag{1.22}$$

where  $L_p$  and  $L_n$  are the minority carrier diffusion lengths in the p and n material, respectively.  $D_n$  and  $D_p$  are the electron and hole diffusion, respectively. From Fermi-Dirac statistics the electron-hole density product is a function of the materials energy gap:

$$np = n_i^2 = N_c N_v \exp(-E_g / kT) \tag{1.23}$$

Where  $N_c$  and  $N_v$  are the conduction and valence band effective density of states, respectively. Therefore the electron to hole injection ratio now becomes a function of the energy gap difference:

$$\frac{J_e}{J_h} = \frac{D_n L_p n_p N_c N_v}{D_p L_n p_n N_c N_v} \exp(\Delta E_g / kT) \tag{1.24}$$

For most compound semiconductor heterostructures, the exponential term in the above equation dominates and a high electron to hole injection efficiency can be achieved as long as the barrier height is sufficient. This nearly ideal single-sided injection of electrons into the active layer makes the double heterostructure GaN/InGaN, and AlGaInP/InGaP LEDs highly efficient. The energy gap differences also minimize the effect of the doping level on the injection efficiency, which dominated the homojunction LED efficiency. Selection of the wide gap

material must take lattice matching into consideration to avoid forming dislocations near the interface that would act as non-radiative recombination centers and therefore significantly reduce the radiative efficiency.

### 1.2.7 Quantum Well LEDs

The quantum well (QW) LED is a special class of heterojunction LED in which the thickness of the active region is less than the deBroglie wavelength of the electron in the semiconducting materials. Basically the electron and hole are confined so tightly in space that discrete energy levels arise due to the wave-particle nature of the electron and hole. This effect causes electrons and holes in the subbands to recombine and emission is blue shifted to larger energies than the bulk DH LEDs. The details of emission in quantum structures are especially important in laser diodes and will be discussed in more detail in later chapters.

## 1.3 LED MATERIALS SELECTION

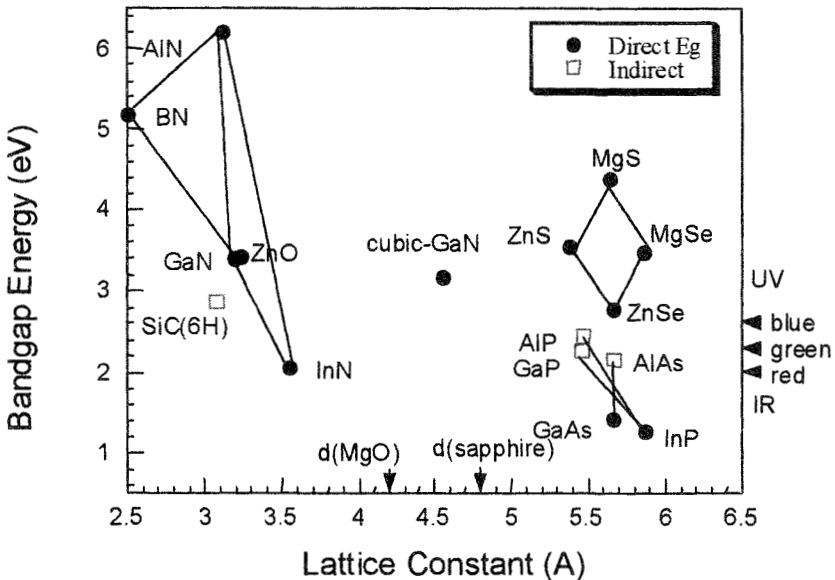


**Figure 1.7** Bandgap energy versus bond length for various semiconductors. Note the general increase in bandgap as the bond length decreases.

### 1.3.1 Energy Band Structure/Lattice Constants

The band gap in the (Al,Ga,In)N based materials system ranges from 1.9eV (InN), 3.4 (GaN) to 6.2 eV (AlN). The band structure is currently thought to be a direct bandgap across the entire alloy range. Therefore, as illustrated in Figure 1.7,

almost the entire visible range and deep UV wavelengths are spanned in the group-III nitride alloy system. This direct bandgap is especially fortuitous as it allows for high quantum efficiency light emitters to be fabricated in the group-III nitride system. Band bowing has not been accurately determined for all the alloys and is therefore not including in the bandgap diagram shown.

### 1.3.2 GaN Physical Properties

The Group-III nitrides possess several remarkable physical properties which make them particularly attractive for reliable solid state device applications. The wide bandgap materials possess low dielectric constants with high thermal conductivity pathways. As shown in Table 1.2 Group-III nitrides exhibit fairly high bond strengths and very high melting temperatures. The large bond strengths could possibly inhibit dislocation motion and improve reliability in comparison to other II-VI and III-V materials. In addition, the nitrides are resistant to chemical etching and should allow GaN based devices to be operated under harsh environments. These properties may lead to a device with superior reliability.

**Table 1.2** Thermal Conductivities energy gaps, bond strengths and mobility of III-V nitrides (Slack, 1973, Sze, 1981 and Harrison, 1980).

	AlN	GaN	InN
K (W/m °K)	320	120	-
Tm (°K)	3500	2800	2150
PN <sub>2</sub> (KBar)	60	45	37
Bond(eV/bond)	2.88	2.2	1.93
Mobility(300K)	-	900cm <sup>2</sup> /Vs	-

### 1.3.3 GaN based LED Structures

Two types of Blue LEDs are commercially available: Laterally contacted devices with 2.5 nm thick single quantum well (SQW) InGaN active regions on sapphire substrates from Nichia Chemical Industries, Ltd., and vertically contacted GaN/AlGaIn double heterostructure (DH) devices on conducting SiC substrates by Cree Research Inc. The laterally contacted device is constructed from a low temperature GaN buffer layer first grown at 550°C, followed by a subsequent n-GaN layer, a 2.5 nm thick InGaN undoped active region, a p-Al<sub>0.1</sub>Ga<sub>0.9</sub>N cladding, and Mg-doped p-GaN layer. Evaporating a p-type contact consisting of NiAu, and a thin NiAu current spreading layer completed the LED process. After chlorine reactive ion etching (RIE) of the mesa, TiAl was evaporated as n-contact metal. The SQW LEDs are extremely efficient currently, the best external efficiency achieved for the blue and green LEDs is 10% and 12% external quantum efficiencies, respectively (Nakamura *et al.*, 1997). The white LEDs are approximately 5% and have a luminous efficacy of 10 lumens/watt, which is becoming competitive with existing incandescent sources. In addition, newly

developed InGaN amber LEDs are superior to conventional AlGaInP amber LEDs in terms of temperature performance. The wavelength shift as a function of temperature is much smaller in GaN than in GaAs based LEDs. Mukai showed a comparison of InGaN to AlGaInP based LEDs at elevated temperature 80°C in which the InGaN LED light output is decreased by only 20%, whereas the AlGaInP LED light output is down by 70% (Mukai *et al.*, 1998). This excellent temperature performance for GaN based LEDs in comparison to conventional

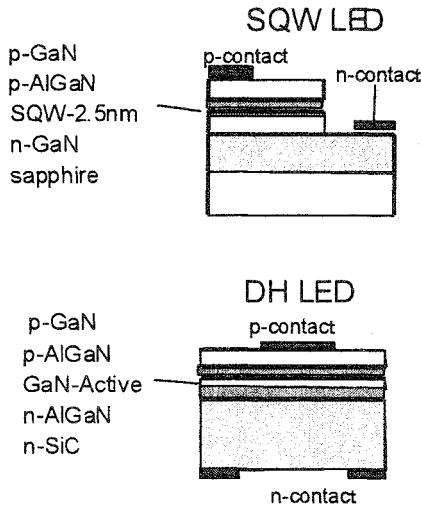


**Figure 1.8** Cross-section of two types of blue GaN LEDs that are commercially available. Because of the increase optical extraction efficiency, a transparent substrate (TS) either sapphire or SiC is employed. The SQW device from Nichia uses lateral current conduction, while CREE uses a vertically conducting buffer layer.

GaAs based LEDs is also seen when comparing to GaP green and AlGaAs red LEDs. The InGaN yellow LEDs are not as bright as transparent substrate (TS) AlGaInP LEDs, but their performance rivals absorbing substrate AlGaInP LEDs. At 20 mA the new yellow LED is 4Candela and has an external efficiency of 3.3 % at 594 nm (Dingle *et al.*, 1994). With these achievements nitride LED's rank among the highest efficiency LED's on the market as shown in Table 1.1 The fundamental improvement in the material quality was attributed in part to the invention of a two-flow MOCVD reactor which features a vertical subflow and horizontal source flow (Nakamura, 1991a). This subflow reduces the boundary layer thickness, thus providing a higher concentration of active nitrogen species at the substrate surface. The evolution of LEDs to efficiency is comparable and in some cases exceeds tungsten light bulbs as shown in Figure 1.5. The bright blue/green GaN LEDs that have been achieved by Nichia are undergoing testing for traffic signal replacement (Nakamura, 1995b). This is a truly remarkable achievement given that the dislocation densities in these LEDs are approximately  $2\text{-}10 \times 10^{10} \text{cm}^{-2}$ . The high defect densities would normally severely reduce any radiative emission from GaAs based LEDs where dislocation densities of about  $10^4/\text{cm}^2$  limit the efficiency (Lester *et al.*, 1995).

The second type of LED structure is grown on SiC substrates and is made by Cree Research Inc. These devices feature a MOCVD grown GaN-AlGaIn p-n junction grown on 6H-SiC substrates. SiC has the advantage of having a smaller lattice misfit to GaN and the possibility of providing n-doped substrates. Another advantage is that the vertical conduction pathway allows for a drop in replacement part similar to the other GaP and GaAs based structures which have the same vertical geometry. The high thermal conductivity of SiC substrates might also benefit the high temperature high output power applications of GaN LEDs. The GaN/SiC output power is lower than that available on sapphire and is commercially available with 0.5 mW and external quantum efficiency of 1.0% (Cree Research Inc., 1995).

A key development in the achievement of high brightness blue LED device structures is the use of the ternary compound InGaIn. High quality films of this alloy allowed the extension of GaN LEDs into the visible spectrum and the ability to use double heterostructure technology. The use of double heterostructure is very effective for obtaining good carrier confinement and single-sided injection into the active layer. Good quality InGaIn was initially demonstrated by Yoshimoto (Yoshimoto *et al.*, 1991) using a high indium source flow and a high growth temperature of 800°C. At these temperatures the high indium source flow is necessary to maintain an overpressure of indium as indium is desorbing from the InGaIn alloy. Nakamura *et al.* further improved the structural and optical quality of InGaIn films using the two-flow MOCVD approach. In the first LEDs, it was reported that Co-doping with Zn and Si was found necessary to extend the LEDs into the blue and blue-green portion of the spectrum. Subsequently, growths of high indium composition in thin single quantum well (SQW) LEDs allowed direct transition in the blue, green and yellow spectral regions (Nakamura *et al.*, 1995a).

## 1.4 CRYSTAL GROWTH

Many techniques have been investigated for the crystal growth of III-V nitride thin films. Recently, metalorganic chemical vapor deposition (MOCVD) and molecular beam epitaxy (MBE) have grown the highest quality GaN based materials.

### 1.4.1 MOCVD Growth

MOCVD is non-equilibrium growth technique, which relies on vapor transport of the precursors and subsequent reactions of group-III alkyls and group-V hydrides in a heated zone. The MOCVD technique originated from the early research of Manasevit (1968) who demonstrated that triethylgallium (TEGa) and arsine deposited single crystal GaAs pyrolytically in an open tube cold-wall reactor. Manasevit and co-workers (Manasevit *et al.*, 1969 and 1979) subsequently expanded the use of this technique for the growth of GaAs<sub>1-y</sub>P<sub>y</sub>, GaAs<sub>1-y</sub>Sb<sub>y</sub>, and Al containing compounds. Composition and growth rate are controlled by precisely controlling the mass flow rate and dilution of the various components of the gas stream. The organometallic group III sources are either liquids, such as trimethylgallium (TMGa) and trimethylaluminum (TMAI), or solids such as

trimethylindium (TMIn). The organometallic sources are stored in bubblers through which a carrier gas (typically hydrogen) flows. The bubbler temperature is to precisely control the vapor pressure over source material. The carrier gas will saturate with vapor from the source and transport the vapor to the heated substrate. The group V sources are most commonly gaseous hydrides, e.g. ammonia  $\text{NH}_3$  for nitride growth. Dopant materials can be metal organic precursors (diethylzinc,  $\text{DEZn}$ , cyclopentadienylmagnesium,  $\text{Cp}_2\text{Mg}$ ) or Hydrides (silane, or disilane  $\text{Si}_2\text{H}_6$ ). The substrate usually rests on a block of graphite called a susceptor that can be heated by a RF coil, resistance heated, or radiantly by a strip heater. An important feature of the MOCVD process is that the walls are kept substantially colder than the heated interior substrate which minimizes wall deposits and reduces reactant depletion effects which hot-walls would cause. The basic MOCVD reaction describing the GaN deposition process is:



However, the details of the reaction are not well known and the intermediate reactions are thought to be complex. Further work is needed to understand the fundamentals of the crystal growth process.

Both atmospheric-pressure and low-pressure MOCVD reactors are employed by various researchers in the growth of GaN. Atmospheric pressure reactors are favored because of the high partial pressures of ammonia, or nitrogen containing precursor is achievable. The majority of the research groups in Japan have utilized atmospheric pressure for this reason. The breakthrough in bright blue LEDs was achieved by Nakamura *et al.* (1994b) using a modified MOCVD system. Nichia Chemistries Inc. has employed a novel two-flow approach that yielded excellent film quality. As shown in figure 1.9, in this reactor sources are supplied from a horizontal inlet, and a vertical subflow then drives the reactants to the growing film surface.

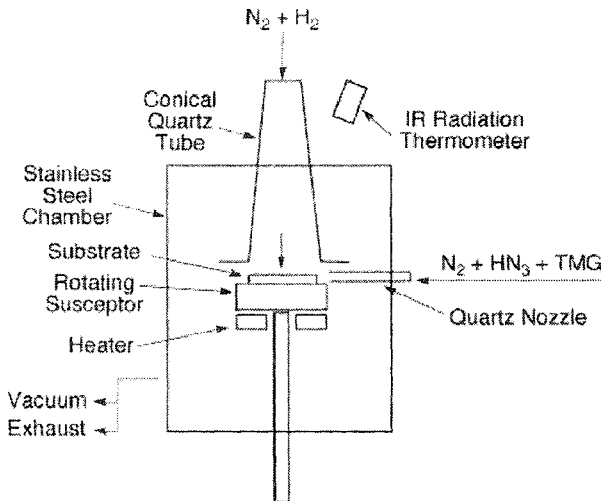
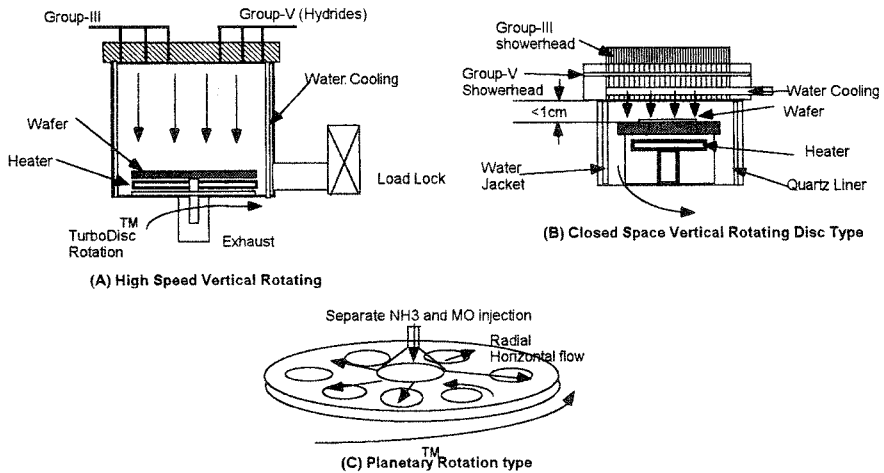


Figure 1.9 Two-flow MOCVD approach (After Nakamura *et al.*)<sup>1</sup>

MOCVD Reactor designs for GaN growth must overcome problems presented by high growth temperatures, pre-reactions, and flow and film non-uniformity. Typically in GaN growth very high temperatures are required because of the high bond-strength of the N-H bond in ammonia precursors. This fact is compounded by the thermodynamic tendency of ammonia to pre-react with the group-III metalorganic compounds to form non-volatile adducts. These factors contribute to the difficulties currently facing researchers in the design and scale-up of III-V nitride deposition systems. Much research activity is needed in the scale-up and understanding of the mechanism of gallium nitride growth by MOCVD.

### 1.4.2 MOCVD Systems for Production

Currently, several types of MOCVD reactor geometries are being developed for the mass production of GaN based materials and devices. Both atmospheric pressure and low-pressure systems are being produced by the major MOCVD equipment manufacturer (Aixtron GmbH, Emcore Corp., Nippon Sanso, and Thomas Swan, Ltd.). Three types of geometries are illustrated in Figure 1.10. This figure shows a high speed rotating disc reactor for LP-MOCVD, a closed space RDR for atmospheric pressure growth, and a two-flow horizontal flow pancake reactor. All three reactor designs are producing high quality GaN materials and it is not the intent of the author to judge one superior to the other. The benefits to each approach will be specific to the ultimate device and materials being grown. For the high speed vertical reactors from Emcore Corporation the main advantage is the large reactor size available (>6 wafers) and the thin uniform boundary layer caused



**Figure 1.10** Three types of MOCVD production reactors for GaN. (a) High speed vertical rotating style (b) Closed space rotating disc type (c) Planetary rotation with radial horizontal flow.

by the high rotation speed (up to 1500 rpm). The closed space RDR has the benefit of atmospheric pressure operation because the low free height eliminates free convection. The two-flow horizontal planetary rotation™ reactor from Aixtron can also be operated at near atmospheric pressure and can accommodate large wafer volumes (>7 wafers). The selection of any reactor has to be carefully considered against factors such as: material quality, high throughput, reproducibility, maintenance, and source usage.

### 1.4.3 Molecular Beam Epitaxy (MBE)

Recently, many researchers have begun developing MBE for growth of the III-V nitrides. Several approaches have been investigated for supplying an atomic source of nitrogen. RF plasma and electron cyclotron resonance (ECR) microwave plasma sources are the two most successful techniques discovered to date (Lei *et al.*, 1991, Strite *et al.*, 1991 and Paisley *et al.*, 1989). In these systems the plasma source is used to crack molecular nitrogen. The plasma sources use a cylindrical cavity geometry to efficiently couple microwave energy into the nitrogen discharge area. The plasma stream is a complex mixture of atomic, molecular, and ionic N radicals. When using ECR sources a tradeoff between growth rate and ion damage has been observed (Lei *et al.*, 1991); under normal ECR use the flux of low energy reactive N species is so low that only low growth rates of 500Å/hr can be achieved. At higher microwave powers high growth rates can be achieved, but ion damage leading to deep levels and semi-insulating electrical properties is observed. Special care must be taken to limit the damage that high energy ionic species might cause if they from reach the surface. Mostakas *et al.*, (1993) have developed a apertured solenoid source which significantly reduced ion damage and enabled them to achieve the first GaN homojunction LED to be grown entirely by MBE (Molnar, 1995). Figure 1.11 shows one type of MBE nitride system that incorporates a nitrogen plasma source to achieve GaN materials. A major advantage of MBE for

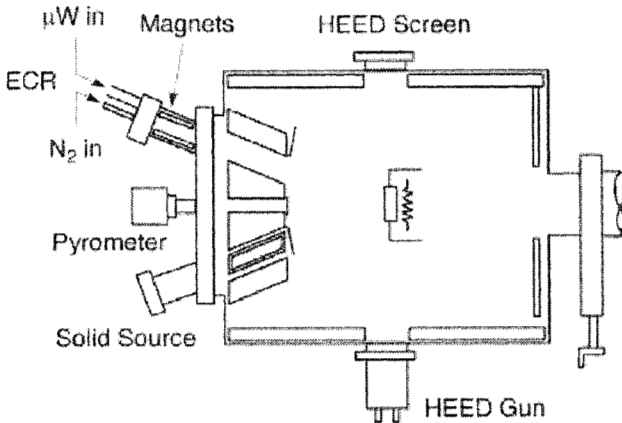


Figure 1.11 MBE nitride system using nitrogen plasma cracking.

nitride growth is the low growth temperature that can be achieved due to the atomic nitrogen source. This is in contrast to MOCVD which must employ high growth temperatures (>1000°C) to crack the ammonia molecules. The lower growth temperature should result in lower thermal stress upon cooling, less diffusion, and reduced alloy segregation. This is especially important in the AlGaIn alloys which possess a large mismatch in the thermal expansion coefficient. Another advantage of MBE is that as-grown p-GaN films by MBE are not passivated due to the absence of atomic hydrogen species during the growth (Mostakas *et al.*, 1993).

#### 1.4.4 Chloride Vapor Phase Epitaxy

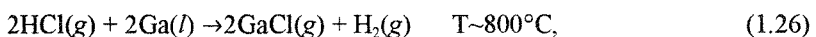
Vapor Phase Epitaxy (VPE) is another technique being investigated for GaN growth. In this technique Cl is used to transport the group-III species instead of organometallic sources. This has a distinct advantage in that large growth rates can be achieved with this technique over the previously described method. In fact Maruska and Tietjen (1969) grew the first high quality GaN thin films. In contrast to MOCVD, which is a non-equilibrium cold-wall reactor based technique, Chloride based VPE is an equilibrium based hot-wall reactor technique.

Very high growth rates of up to 40 μm/hr can be achieved with the VPE technique. This has potential to generate thick GaN layers to actually form substrates. Akasaki *et al.* has used this technique to grow thick films on ZnO/Sapphire substrates and subsequently lift-off the layers and thus create a thick vapor deposited GaN “substrate”. Considerable research is needed to control In segregation by VPE so that this technique can be applied to the InGaIn alloys.

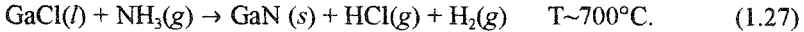
VPE relies on the gaseous transport of the constituent column III and column V sources to the deposition zone. Mass flow controllers achieve precise control of the molar flowrates of the two column V source. This allows independent control of the partial pressures that govern alloy composition grading. A high degree of flexibility in the composition and doping levels is achieved by accurate mass flow control. The versatile nature of VPE allows synthesis of the important III–V compounds such as GaN, ZnAs, GaP, InGaP, InAsP, and GaAsSb. However, the important ternary Al<sub>x</sub>Ga<sub>1-x</sub>As compounds and more importantly AlGaIn compounds cannot be grown by VPE since the AlCl species reacts with the hot quartz walls resulting in unwanted impurities in the epitaxial film (Kressel, 1977a).

In contrast to MOCVD, Hydride-VPE is a reversible equilibrium based process in which the crystal growth is achieved by lowering the growth temperature of the substrate relative to the temperature of the reaction zone. For GaAs<sub>1-x</sub>P<sub>x</sub> growth the Ga reservoir portion of the furnace is held at approximately 800°C. GaCl is formed by introducing a mixture of HCl and H<sub>2</sub> to the Ga reservoir. The reaction zone is kept at 1100°C to pyrolyze the hydrides NH<sub>3</sub>. During deposition the substrate is kept at a lower temperature of approximately 750°C so that the vapor becomes supersaturated and deposition occurs.

The hydride-VPE process can be described by the following set of chemical reactions: gallium transport by chloride formation in the gallium zone:



transport and reaction with the hydrides in the reaction zone:



Ammonia is then thought to decompose at the surface and react with either GaCl or Ga to form GaN. However, further work on VPE reaction mechanisms is needed to clarify the reaction pathways. One of the main advantages of VPE is the ease of scale-up to a high capacity commercial process.

## 1.5 GROUP-III NITRIDE MATERIALS GROWTH ISSUES

Several major breakthroughs in the MOCVD growth of high quality GaN and InGaN enabled the fabrication of device quality group-III nitride materials. In this section we will discuss several of these key growth issues such as: (i) Substrates and the implementation of low temperature nucleation layers to provide a homogeneous nucleation on the sapphire substrates (Hiramatsu *et al.*, 1991), (ii) the achievement of p-type doping in GaN by overcoming the hydrogen passivation of acceptors (Amano *et al.*, 1989 and Nakamura *et al.*, 1992a), (iii) Growth of GaN, AlGaIn, and InGaIn with high optical and electrical quality and (iv) growth of GaN/InGaIn heterostructures and quantum wells.

### 1.5.1 Substrates

Several problems in the epitaxial growth of nitrides originate from the non availability of single crystalline GaN substrates or other high quality single crystalline substrates with the same lattice parameters as GaN. For this reason, so far, most of the epitaxial growth of nitrides has been performed on sapphire or SiC substrates. In both cases, problems due to the lattice mismatch between the nitride epi-layer and the substrate (16% for sapphire and 3.5 % for SiC) have to be overcome. One of the major breakthroughs in the growth of device quality group-III nitride material was the implementation of nucleation layers. Using sapphire substrates, thin AlN or GaN nucleation layers deposited at temperatures between 500 and 750°C showed to remarkably improve the quality of the GaN film grown at temperatures above 1000°C (Akasaki, *et al.* 1989 and Nakamura, 1991b). In the case of SiC substrates, the growth is usually initiated with the deposition of a thin AlN nucleation layer at high temperatures (Weeks *et al.*, 1995).

By this means, GaN material of comparable quality on both types of substrates could be achieved. Since so far, most GaN growth has been performed on c-plane sapphire substrates, in the following section just the growth on c-plane sapphire will be discussed.

Additional substrate materials are currently being examined to determine if the properties of the GaN thin films can be enhanced by improved structural matching. From Figure 1.7 we can see that in addition to sapphire several other substrates offer potentially much better latticed and thermal matching. To this end, 6H-SiC, ZnO, and 3C-SiC, MgO are alternative substrate materials. ZnO has a wurtzite structure with lattice constants of ( $a=3.32\text{\AA}$ ,  $c=5.213\text{\AA}$ ) and thus offers a

better structural match to the equilibrium wurtzite nitride. 3C-SiC and MgO are both cubic zinc-blende structures having better structural and thermal match to the nitrides than sapphire. 3C-SiC and MgO have cubic lattice constants of  $a=4.36\text{\AA}$  and  $a=4.22\text{\AA}$ , respectively. Although the nitrides are most commonly observed as the wurtzite (2H) polytype, they can also crystallize in a metastable zinc-blende structure ( $a=4.52\text{\AA}$ ) when using non-equilibrium based growth techniques. The identification of a suitable substrate material that is lattice matched and thermally compatible with GaN wurtzite structure ( $a=3.19\text{\AA}$ ,  $c=5.185\text{\AA}$ ) will alleviate many of the difficulties associated with the deposition of device quality material.

### 1.5.2 Nucleation Layer technology

The deposition of a low temperature "buffer" layer of AlN on sapphire substrates was a key discovery in improving surface morphology and crystalline quality of GaN. Yoshida *et al.* (1983) was the first to recognize the importance of depositing a low temperature buffer layer. The surface morphology of the subsequent thick GaN layers can be markedly improved if thickness of the buffer layer is optimized. Subsequent work by Akasaki *et al.* (1988) resulted in significantly improved nitride films in which stimulated band-edge emission was observed (Amano *et al.*, 1990b). In this work it was reported that the AlN buffer layer relaxes the strain between GaN and sapphire, and promotes lateral growth of GaN. TEM results show that the buffer layer is highly dislocated and subsequent layers have a much lower dislocation density.

Structural characterization by transmission electron microscopy (TEM), atomic force microscopy (AFM), and high resolution X-ray diffractometry (XRD) revealed that the nitridation of the sapphire substrate plays an important role in controlling the defect structure and therefore dislocation densities in overgrown GaN films (Heying *et al.*, 1995). Based on these material studies, the understanding of X-ray rocking curves and their correlation with nucleation processes, material properties and defect structures in GaN films on sapphire was elucidated. It has been reported that changing the nitridation time of the sapphire surface before growth initiation results in a variation of the overall dislocation density between  $10^{10}$  and  $10^8\text{cm}^{-2}$ . Based on these comprehensive structural characterizations, GaN thin films with record low dislocation densities of  $1.7 \times 10^8\text{cm}^{-2}$ .

### 1.5.3 Growth and doping of GaN

The best reported mobility for bulk GaN is by Nakamura *et al.* (1992b), in which a mobility of 900 at 300K and a low free carrier concentration of  $2 \times 10^{16}\text{cm}^{-3}$  were observed. Exact defect density in these films is not known. In our studies the best films were nominally undoped 4  $\mu\text{m}$  thick GaN films in which we observed 300 K mobilities of  $780\text{cm}^2/\text{Vs}$  ( $n:300\text{K} = 6 \times 10^{16}\text{cm}^{-3}$ ). On these samples dislocation densities of  $4 \times 10^8\text{cm}^{-2}$  for GaN on sapphire substrates was observed in cross-sectional TEM measurements (Kapolnek *et al.*, 1995). Even at excitation levels as low as  $2.2\text{mW/cm}^2$ , the 300K PL is dominated by the near band edge emission .

One of the key breakthroughs in the development of GaN technology was the achievement of p-doping using Mg and LEEBI treatment. Amano (Akasaki *et al.*, 1989) observed that under low electron beam irradiation (LEEBI) Mg-doped GaN exhibited much lower resistivity and the PL properties drastically improved. This achievement subsequently led to the development of p/n GaN diodes with good turn on characteristics. Nakamura *et al.* (1993) built upon this fundamental breakthrough to achieve even higher p-doping and uniform activation of Mg by using high temperature thermal annealing under a nitrogen ambient. The passivation requires post growth treatment for MOCVD material to activate the dopants. During the growth, interstitial hydrogen is incorporated and a H-Mg acceptor complex forms which passivates the acceptor. This H-Mg bond can be broken by a high temperature annealing step under an inert environment. This work demonstrated that hydrogen compensation of Mg in the MOCVD growth of GaN was the principal problem that plagued previous researchers. High room temperature p-doping is further complicated by the high activation energy of Mg as the most commonly used dopant (270 meV) and the passivation of acceptors with hydrogen during CVD growth. The binding energies of dopants are dependent of the dielectric constant and effective mass of the material. The nitride system has low dielectric constant (GaN,  $\epsilon(0)=9.5$ ) and large effective masses (GaN,  $m_e=0.2m_0$ ,  $m_h=0.75m_0$ ) resulting in large binding energies. This is especially pronounced in p-type doping, when comparing GaN to GaAs the acceptor levels are very deep because of the large hole mass. This has led to difficulties in high p-type doping. This is the result of two effects: high n-type background concentration compensating the p-dopant and the incomplete activation of the dopants at room temperature. The low p-type doping (typical values are  $10^{17}\text{cm}^{-3}$ ) leads to high contact resistances and problems with current spreading. Further work on increasing the p-doping level and developing new p-dopants will result in substantial payoff in producing LEDs and lasers with lower operating voltages and higher power efficiencies.

Doping n-type is rather straightforward in GaN with silicon being the typical n-dopant. The as-grown material is a typical unintentionally n-type, which is widely believed to be due to intrinsic nitrogen vacancies. The Si donor lies just below the conduction band ( $E_a=15\text{-}25$  meV). Therefore well-controlled n-type doping can be easily accomplished using silicon as the donor. The typically MOCVD precursor for n-type doping are silane ( $\text{SiH}_4$ ) and disilane ( $\text{Si}_2\text{H}_6$ ) which are typically diluted with hydrogen in the 200ppm range. Doping levels between  $1\times 10^{17}$  to  $2\times 10^{19}\text{cm}^{-3}$  are easily achieved in the doping of GaN with silane.

### 1.5.4 Growth of AlGaN and AlGaN/GaN Heterostructures

High quality AlGaN films have been demonstrated by atmospheric pressure MOCVD as well as epitaxy performed under low pressure conditions. Parasitic reactions between TMAI and  $\text{NH}_3$  are much more likely to occur than with TMGa. Two-flow-channel reactors with separate injection of the Group-III and Group-V precursors or reactor operation under low pressure conditions have been shown to successfully prevent excessive pre-reactions in the gas phase.

At growth temperatures below 1100°C, the mole fraction of aluminum in the AlGaIn epitaxial layer was found to be almost directly proportional to the mole fraction of TMAI in the gas phase. At temperatures above 1100°C, the incorporation efficiency of gallium atoms decreased. This behavior was explained by a decreased sticking probability of Ga molecules at this high temperatures (Hirosawa *et al.*, 1993). K. Sayyah *et al.* (1986) reported on a decrease of the gallium incorporation efficiency with increasing TMAI flow and explained this behavior by an surface kinetic model and competitive adsorption. The same authors found an decrease of the gallium incorporation efficiency with increasing SiH<sub>4</sub> dopant flow also (Sayyah, *et al.*, 1986).

High quality AlGaIn/GaN heterostructures are characterized by a very high mobility of the two dimensional electron gas at the interface (Kahn *et al.*, 1991) Values as high as 1500cm<sup>2</sup>/Vs at room temperature have been achieved in the authors' laboratory (Wu *et al.*, 1996). The optical properties of AlGaIn/GaN quantum wells (Kahn, *et al.*, 1990) were found to be determined by both quantum and strain related effects (Krishnankutty *et al.*, 1992a and 1992b). MOCVD AlN films showed a full width of half maximum of the (002) X-ray rocking curve peak as low as 97 arcseconds (Saxler *et al.*, 1994). AlN/GaN Superlattices of high structural and optical quality have also been fabricated by switched atomic layer MOCVD (Kahn *et al.*, 1993).

### 1.5.5 Growth of InGaIn and InGaIn/GaN Heterostructures

Growth of high quality InGaIn is necessary to obtain good electrical and optical characteristics from LEDs. However, the growth of high quality InGaIn has proven to be more difficult than GaIn. InGaIn growth needs to be performed at much lower temperatures than that of GaIn, due to the low dissociation temperature of InN (Matsuoka *et al.*, 1988 and Koukitsu *et al.*, 1996). Furthermore, the decomposition of ammonia becomes less efficient with decreasing temperature due to the high kinetic barrier for breaking the nitrogen-hydrogen bonds. The growth of InGaIn has to be performed at temperatures below 850°C because of the high volatility of indium at common GaIn growth temperatures of above 1000°C. But even on InGaIn layers grown at temperatures below 800°C, indium droplet formation was observed (Shimizu *et al.*, 1994).

The indium incorporation into the InGaIn films strongly increases with decreasing growth temperature. Also, the relative indium incorporation coefficient  $k_{In}$ , defined as:

$$k_{In} = x_{S_{In}} \times f_{TMGa} / (1 - x_{S_{In}}) \times f_{TMIn}. \quad (1.28)$$

( $x_S$ : In-In composition in the solid) increases with increasing growth rate at a given temperature, as shown in Figure 1.12. This indicates, that the incorporation of indium is limited by the evaporation of indium species from the surface. The tendency for evaporation decreases at lower temperature and/or increasing growth rate, when the indium species become trapped by the growing layer. But at growth temperatures below 760°C, high quality InGaIn films could be obtained only by reducing the growth rate to values equal or lower than 3 Å/s in the authors' reactor.

These films showed intense band edge related luminescence at room temperature (Varon et al., 1981). The full width at half maximum (FWHM) of the X-ray diffraction peaks was 6.1 and 6.6 arcmin for layers containing 9% and 20% indium, respectively.

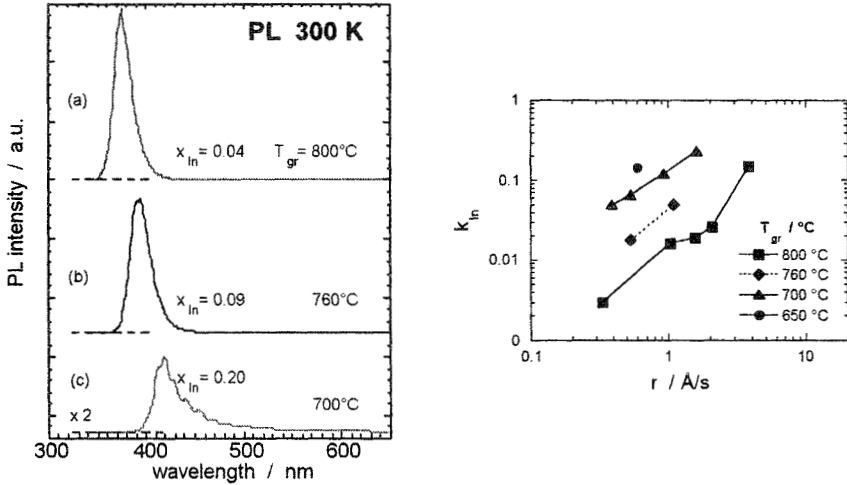


**Figure 1.12** Effect of temperature on (a) PL wavelength and (b) Indium incorporation coefficient. Lower temperatures and higher growth rates result in higher indium incorporation.

## 1.6 CONCLUSIONS

The Group-III nitride semiconductors have emerged as the leading material for fabricating high efficiency and high reliability short wavelength emitters. MOCVD has emerged as the leading growth technology for depositing high quality GaN/InGaN heterostructure based devices. Well controlled doping, low background carrier concentrations, and high mobilities exceeding  $800\text{cm}^2/\text{Vs}$  has been demonstrated by several research groups. The use of low temperature ( $500\text{--}600^\circ\text{C}$ ) GaN buffer layers and p-type GaN has resulted in high crystalline quality material on sapphire. Optimization of the MOCVD growth of InGaN/GaN based quantum structures has enabled high efficiency blue LEDs and laser diodes to be achieved. GaN based blue LEDs with external quantum efficiencies of 10% and 5mW output power at 20mA have recently been demonstrated, and are bright enough for full-color outdoor displays.

**1.7 REFERENCES**

- Akasaki, I., Amano, H., 1988, *Appl. Phys. Lett.* **56**, p. 185.
- Akasaki, I., Amano, H., Koide, Y., Hiramatsu, K. and Sawaki, N., 1989, *J. Cryst. Growth*, **89**, p. 209.
- Amano, H., Sawaki, N., Akasaki, I. and Toyoda, Y., 1986, *Appl. Phys. Lett.* **48**, p. 353.
- Amano, H., Kito, M., Hiramatsu, K. and Akasaki, I., 1989, *Jpn. J. Appl. Phys. Part II*, **28** (12), p. L2112.
- Amano, H., Kitoh, M., Hiramatsu, K. and Akasaki, I., 1990a, *Gallium Arsenide and Related Compounds 1989*, (eds.) Ikoma, T., Watanabe, H., Bristol, UKIOP, p. 725.
- Amano, H., Asaki, T. and Akasaki, I., 1990b, *Jpn. J. Appl. Phys. Lett.*, **29**, p. 205.
- Capasso, F., Ripamonti, G., Tsang, W. T., Hutchinson, A. L. and Chu, S. N. G., 1989, *J. Appl. Phys.*, **65**(1), p. 388.
- Casey, H.C. and Panish, M., 1978, *Heterostructure Lasers*, Academic Press, New York.
- Craford, M.G., 1977, *IEEE Trans. Electron. Devices*, ED-**24**, p. 935.
- Cree Research Inc., 1995, *Product Specification Sheet*, Super Blue LED C430-DH85.
- Dingle, D., Shaklee, K.L., Leheny, R.F. and Zetterstrom, R.B., 1994, *Appl. Phys. Lett.*, **64**, p. 1377.
- Harrison, W.A., 1980, *Elec. Structure and Properties of Solids Ed.* Freeman (San Francisco).
- Henry, C.H. et al., 1976, *J. Luminescence*, **12/13**, p. 47.
- Heying, B., Wu, X.H., Keller, S., Li, Y., Kapolnek, D., Keller, B., DenBaars, S.P. and Speck, J.S., 1995, *Appl. Phys. Lett.*, **68**(5) p. 643.
- Hiramatsu, K., Itoh, S., Amano, H., Akasaki, I., Kuwano, N., Shiraishi, T. and Oki, K., 1991, *J. Cryst. Growth*, **115**, p. 628.
- Hirosawa, K., Hiramatsu, K., Sawaki, N. and Akasaki, I., 1993, *Jpn. J. Appl. Phys.*, **32**, p. L1030.
- Holynak, Jr. N. and Bavacqua, S.F., 1962, *Appl. Phys. Lett.*, **1**, p. 82.
- Kahn, M.A., Skogman, R.A., Van Hove, J.M., Krishnankutty, S. and Kolbas, R.M., 1990, *Appl. Phys. Lett.*, **56**, p. 1257.
- Kahn, M.A., Van Hove, J.M., Kuznia, J.N. and Olson, D.T., 1991, *Appl. Phys. Lett.*, **58**, p. 2408.
- Kahn, M.A., Kuznia, J.N., Olson, D.T., George, T. and Pike, W.T., 1993, *Appl. Phys. Lett.*, **63**, p.3470.
- Kapolnek, D., Wu, X.H., Heying, B., Keller, S., Keller, B.P., Mishra, U.K., DenBaars, S.P. and Speck, J.S., 1995, *Appl. Physics. Lett.*, **67** (11) p. 1541.
- Koukitsu, A., Takahashi, N., Taki, T. and Seki, H., 1996, *Jpn. J. Appl. Phys.*, **35**, p. L673.
- Kressel, M., 1977a, *Semiconductor Lasers and Heterojunction LEDs*, Academic Press, New York.
- Kressel, M., et al., 1977b, Academic Press, NY, p. 294.
- Kressel, M., et al., 1977c, Academic Press, NY, p. 295.
- Krishnankutty, S. and Kolbas, R.M., Kahn, M.A., Kuznia, J.N., Van Hove, J.M. and Olson, D.T., J, 1992a, *Electron. Mat.*, **21**, p. 437.

- Krishnankutty, S. and Kolbas, R.M., Kahn, M.A., Kuznia, J.N., Van Hove, J.M. and Olson, D.T., J, 1992b, *Electron. Mat.*, **21**, p. 609.
- Kroemer, H., 1963, *Proc. IEEE*, **51**, p. 1782.
- Lei, T., Fanciulli, M., Molnar, R.J., Moustakas, T.D., Graham, R.J. and Scanlon, J.D., 1991, *Appl. Physics Lett.*, **59**, p. 94.
- Lester, S.D., Ponce, F.A., Craford, M.G. and Steigerwald, 1995, D.A., *Appl. Phys. Lett.*, **66**, p. 1249.
- Manasevit, H.M., 1968, *Appl. Phys. Lett.*, **12**, p. 156.
- Manasevit, H.M. and Simpson, W.I., 1969, *Electrochem. Soc.*, **116**, p. 1725.
- Manasevit, H.M. and Hess, K.L., 1979, *J. Electrochem. Soc.*, **126**, p. 2031.
- Maruska, H.P. and Tietjen, J.J., 1969, *Appl. Physics Lett.* **15**, p. 327.
- Matsuoka, T., Tanaka, H., Sasaki, T. and Katsui, A., 1988, *Inst. Phys. Conf. Ser., No 106, GaAs and related compounds*, chapter 3, p.141.
- Molnar, R.J., Singh, R. and Mostakas, T., 1995, *Appl. Phys. Lett.*, **66**(3) p. 268.
- Mostakas, T.D. and Molnar, R.J., 1993, *Mater. Res. Soc. Proc.*, **281**, p. 753.
- Mukai, S., Narimatsu, H. and Nakamura, S., 1998, *Jpn. J. Appl. Phys. Part 2*, **37**, p. L479.
- Nakamura, S., 1991a, *Jpn. J. Appl. Phys.*, **30**, p. 1620.
- Nakamura, S., 1991b, *Jpn. J. Appl. Phys.*, **30**, p. L1705.
- Nakamura, S., Iwasa N., Senoh M. and Mukai T., 1992a, *Jpn. J. Appl. Phys.*, **31**, p. 1258.
- Nakamura, S., Mukai T. and Senoh M., J. 1992b, *Appl. Phys.*, **71**, p. 5543.
- Nakamura, S., Senoh M. and Mukai T., 1993, *Jpn. J. Appl. Phys.*, **32**, p. L8.
- Nakamura, S., Mukai T. and Senoh M., 1994a, *Appl. Phys. Lett.*, **64**, p. 1687.
- Nakamura, S., Mukai T. and Senoh M., March 1994b, *Appl. Phys. Lett.*, **64**, p. 1687.
- Nakamura, S., Iwasa N., Senoh M., Nagahama, S., Yamada, T. and Mukai T., 1995a, *Jpn. J. Appl. Phys. Lett.*, **34**, p. L1332.
- Nakamura, S., 1995b, private communication, Feb.
- Nakamura, S. and Fasol, G., 1997, *The Blue Laser Diode*, Springer-Verlag, Heidelberg, Germany.
- Paisley, M.J., Sitar, Z., Posthill, J.B. and Davis, R.F., 1989, *J. Vac. Sci. Technol.*, **A7**, p. 701.
- Pankove, J.I., Miller, E.A. and Berkeyheiser, J.E., 1971, *RCA Rev.*, **32**, p. 383.
- Saxler, A., Kung, P., Sun, C.J., Bigan, E. and Razeghi, M., 1994, *Appl. Phys. Lett.*, **64**, p. 339.
- Sayyah, K., Chung, B.-C. and Gershenson, M., 1986, *J. Cryst. Growth*, **77**, p. 424.
- Shimizu, M., Hiramatsu K. and Sawaki, N., 1994, *J. Cryst. Growth*, **145**, p. 209.
- Shockley, W., 1950, *Electrons and Holes in Semiconductors*, Van Nostrand Co., New York.
- Slack, G.A., 1973, *Phys. Chem. Solids*, **34**, p. 321.
- Strite, S., Ruan, J., Li, Z., Manning, N., Salavador, A., Chen, H., Smith, D.J., Choyke, W.J. and Morkoc, H., 1991, *J. Vac. Sci. Technol.*, **B9**, p. 1924.
- Sze, S.M., 1981, *Physics of Semiconductor Devices*, p. 849.
- Varon, J. et al. 1981, *IEEE Trans. Electron. Dev.*, **4**, p. 416.
- Weeks, Jr. T. W., Bremser, M.D., Ailey, K.S., Carlson, E., Perry, W.G. and Davis, R.F., 1995, *Appl. Phys. Lett.* **67**, p. 401.